Comparison of Near-Surface Air Temperatures and MODIS Ice-Surface Temperatures at Summit, Greenland (2008–13)

CHRISTOPHER A. SHUMAN

Joint Center for Earth Systems Technology, University of Maryland, Baltimore County, Baltimore, and NASA Goddard Space Flight Center, Greenbelt, Maryland

DOROTHY K. HALL

Cryospheric Sciences Laboratory, NASA Goddard Space Flight Center, Greenbelt, Maryland

NICOLO E. DIGIROLAMO

Science Systems and Applications, Inc., and NASA Goddard Space Flight Center, Greenbelt, Maryland

THOMAS K. MEFFORD

Cooperative Institute for Research in Environmental Sciences, University of Colorado Boulder, and NOAA/Earth System Research Laboratory, Boulder, Colorado

MICHAEL J. SCHNAUBELT

Joint Center for Earth Systems Technology, University of Maryland, Baltimore County, Baltimore, Maryland

(Manuscript received 7 January 2014, in final form 30 June 2014)

ABSTRACT

The stability of the Moderate Resolution Imaging Spectroradiometer (MODIS) ice-surface temperature (IST) product from *Terra* was investigated for use as a climate-quality data record. The availability of climate-quality air temperature data T_A from a NOAA observatory at Greenland's Summit Station has enabled this high-temporal-resolution study of MODIS ISTs. During a >5-yr period (July 2008–August 2013), more than 2500 IST values were compared with ±3-min-average T_A values from NOAA's primary 2-m temperature sensor. This enabled an expected small offset between air and ice-sheet surface temperatures (T_A > IST) to be investigated over multiple annual cycles. The principal findings of this study show 1) that IST values are slightly colder than the T_A values near freezing but that this offset increases as temperature decreases and 2) that there is a pattern in IST–T_A differences as the solar zenith angle (SoZA) varies annually. This latter result largely explains the progressive offset from the in situ data at colder temperatures but also indicates that the MODIS cloud mask is less accurate approaching and during the polar night. The consistency of the results over each year in this study indicates that MODIS provides a platform for remotely deriving surface temperature data, with the resulting IST data being most compatible with in situ T_A data when the sky is clear and the SoZA is less than ~85°. The ongoing development of the IST dataset should benefit from improved cloud filtering as well as algorithm modifications to account for the progressive offset from T_A at colder temperatures.

1. Introduction

There has been much attention paid to the increasing ice melt in Greenland, especially related to recently observed warm events and associated unusual climate conditions (Nghiem et al. 2012; Hall et al. 2013; Hanna et al. 2014), the positive ice–albedo feedback (Box et al. 2012), and overall climate conditions (Steffen and Box 2001; Rennermalm et al. 2013). Climate models predict continued Arctic warming, but they differ in their predictions of the extent, rate, and magnitude of the temperature increases. The most practical way to get a spatially broad and temporally extensive measurement

Corresponding author address: Christopher A. Shuman, Joint Center for Earth Systems Technology, University of Maryland, Baltimore County, Code 615, Greenbelt, MD 20771.
E-mail: christopher.a.shuman@nasa.gov

DOI: 10.1175/JAMC-D-14-0023.1

TABLE 1. Summary statistics for the IST–T_A differences for each year.

Year	No. of points	Min (°C)	Max (°C)	Mean (°C)	Std dev (°C)	RMS (°C)
2008* all	222	−27.42	3.08	−3.81	4.01	5.52
2008* filt.	200	−8.49	1.84	−3.01	2.06	3.65
2009 all	535	−29.72	3.50	−3.44	3.77	5.10
2009 filt.	490	−9.44	1.87	−2.70	2.15	3.45
2010 all	474	−26.46	5.43	−3.75	3.98	5.47
2010 filt.	418	−9.21	1.72	−2.85	2.13	3.56
2011 all	510	−34.78	4.04	−3.89	4.60	6.02
2011 filt.	448	−9.74	1.04	−2.82	2.29	3.63
2012 all	488	−20.57	4.10	−3.48	3.62	5.02
2012 filt.	442	−9.99	2.11	−2.82	2.19	3.57
2013* all	307	−24.73	5.90	−1.96	3.48	3.99
2013* filt.	272	−9.13	2.39	−1.88	2.42	3.06

* Indicates that the NOAA Logan sensor observations began on 6 July 2008 and data have been compared through 31 August 2013. Each year of data in the comparison was examined before and after applying a ±5° regression filter to the data (''all'' and ''filt.,'' respectively). See text for the rationale for applying the filter.

of surface temperature for an area the size of the Greenland Ice Sheet (GrIS) is through satellite remote sensing given the difficulties of operating equipment reliably in harsh polar conditions. However, the uncertainties in satellite-derived ice-surface temperatures (ISTs) must be assessed relative to independent air temperature T_A datasets such as those from well-calibrated automatic weather stations (AWS) to validate them for use in climate studies. Full confidence in these remote sensing records can be established by comparison with the best available in situ data.

This research provides an additional assessment of the uncertainties in these multiyear MODIS-derived surface temperatures. Preliminary results have been presented in Hall et al. (2008a, 2012) and Koenig and Hall (2010) for a restricted period of time and temperature range. In those studies, a 1°–3°C ''cold bias'' was identified at Summit using thermocrons (i.e., small temperature loggers) placed on the snow surface during the winter of 2008/09 (Koenig and Hall 2010). In this work, we assess satellite-derived ''clear sky'' IST data from the Moderate Resolution Imaging Spectroradiometer (MODIS) near Summit Station, Greenland (see online at http://modis-snow-ice.gsfc.nasa.gov/index.php?c=greenland). These IST data from July 2008 through August 2013 are compared with 2-m T_A data from the Temporary Atmospheric Watch Observatory (TAWO). This facility has been operated at Summit Station since 2005 by the National Oceanic and Atmospheric Administration (NOAA)/Earth System Research Laboratory Global Monitoring Division (GMD; see online at http://www.esrl.noaa.gov/gmd/obop/sum/). This analysis approach is justified even though air and surface temperatures are not the same (e.g., Hudson and Brandt 2005) because of the quality and high temporal resolution of the NOAA T_A data. The overlap period between the MODIS temperature record and the NOAA Logan Enterprises, Inc., temperature sensor record began at Summit in July of 2008 (see Table 1) and is ongoing.

2. Background

Surface and air temperatures on the GrIS have been studied using AWS data at the ground (e.g., Steffen and Box 2001; Shuman et al. 2001; Box 2002; van den Broeke et al. 2008, 2011) and using satellite data (e.g., Key and Haefliger 1992; Stroeve and Steffen 1998; Comiso 2006; Wang and Key 2005a,b; Comiso 2006; Hall et al. 2008a,b; Hall et al. 2009, 2013). Modeling results (e.g., van den Broeke et al. 2011; Cullather et al. 2014) as well as reanalysis products that ingest data from some in situ sensors (Lucas-Picher et al. 2012) are also available. For a variety of reasons, including the remote and difficult environment, calibration issues, equipment maintenance problems, snow/ice accumulation, and/or power limitations, deriving accurate, extensive, and internally consistent climate-quality temperature records for ice-sheet locations remains a challenge.

IST has been derived from IR channels on various satellites. The primary instruments for which such IR data have been available are the Advanced Very High Resolution Radiometer (AVHRR) on NOAA's Polar-Orbiting Operational Environmental Satellites and MODIS on the National Aeronautics and Space Administration's (NASA) *Terra* and *Aqua* satellites, as well as *Landsat-7*'s Enhanced Thematic Mapper Plus (ETM+, band 6) and also *Terra*'s Advanced Spaceborne Thermal Emission and Reflection Radiometer (ASTER). These sensors have recently been augmented by the Visible Infrared Imaging Radiometer Suite (VIIRS) instrument on the Suomi National Polar-Orbiting Partnership satellite and the Thermal Infrared Sensor (TIRS) on *Landsat-8*.

Hall et al. (2008a) documented that the orbiting IR sensor data available at that time from ETM+, ASTER, and MODIS had very similar performance on the GrIS, with an RMS error of 2.1°C. The clear-sky limitation of satellite-derived IR temperatures precludes the measurement of the surface under all-weather conditions, however. Cloud-top temperatures tend to be colder than surface temperatures because air temperatures tend to fall through the lower atmosphere with increasing altitude (Westermann et al. 2012). Further, orbit characteristics of each satellite allow particular locations to be sampled only during a specific period on any given day. The surface temperature of the ice sheet beneath clouds can be very different, and usually higher, than that under clear skies (e.g., Miller 1956; Stroeve and Steffen 1998; Hudson and Brandt 2005), especially in the winter when there are inversions in the lower atmosphere (Miller et al. 2013). Thus, a time series of satellite-derived, clear-sky, surface temperatures can be significantly different from an all-sky surface temperature record (Liu et al. 2009; Koenig and Hall 2010). Initial comparisons between IST and snow-surface temperature data from thermochrons (a type of programmable thermistor) are presented in Koenig and Hall (2010) and Hall et al. (2012). Those comparisons of temporally similar temperatures during November 2008–February 2009 identified a ~3°C cold bias in the IST data for Summit. Hudson and Brandt (2005) documented a similar offset using in situ sensor data in Antarctica.

a. NOAA 2-m air temperatures

Although preceded by a series of AWS installed in support of the Greenland Ice Sheet Program 2 (GISP2) deep-core and ancillary research projects (Stearns and Weidner 1990; Shuman et al. 2001), climate-quality measurements began in 2005 after the GISP2 camp became Summit Station and also a year-round research facility. Although preliminary measurements began in 2005, NOAA began operating the TAWO facility as part of GMD in 2007. GMD initially used a Vaisala, Inc., sensor in an aspirated Met One Instruments, Inc., housing at TAWO. In July of 2008, a more accurate Logan temperature sensor was installed and now operates in parallel with the Vaisala sensor at TAWO; both sensors are currently in aspirated "Cambridge" housings. At Summit, as at its other GMD sites, NOAA utilizes a Logan PT139 sensor that is factory calibrated using industry-traceable equipment across the expected temperature range for the site (online at http://www.loganent.com/products.php?p=32: see "Platinum Sensor Data"). Further, using International Temperature Scale of 1990 (ITS-90) standards, NOAA/GMD protocols are then applied across the resistances corresponding to a temperature range from −75° to +5°C to achieve temperature accuracies of better than 0.1°C, which are then rounded off to this resolution for the Summit data. In an operational setting, the sensors acquire T_A data 4 times per minute and those values are averaged to 1 min and, as in this study, more typically for longer periods. Onsite personnel are scheduled to maintain the temperature sensors on a daily basis to ensure proper ventilation, and the sensor arm is raised every year to maintain the 2-m offset from the ice-sheet surface. The availability of power year-round at the station means that these sensors can be continually ventilated, unlike most AWS temperature sensors, which are typically not ventilated. There may be occasional adverse impacts as a result of power or other equipment problems. Active ventilation of the T_A sensors avoids some data-quality issues such as solar heating during periods of low wind speed and high insolation that have been quantified for more typical but passively ventilated AWS temperature sensors used on ice sheets (Shuman et al. 2001; Genthon et al. 2011).

b. MODIS ice-surface temperatures

The IR-derived temperatures from MODIS or other sensors (e.g., Key and Haefliger 1992; Comiso 2006; Hall et al. 2008a) represent a skin temperature and not an air temperature. Skin temperature is the temperature of the surface at radiative equilibrium or the temperature essentially at the interface between the snow/ice surface and the atmosphere for a site like Summit Station (Warren and Brandt 2008). This explains some of the differences between IST and T_A that were identified in this study and are discussed further below. As described in detail by Hall et al. (2012), IST can be mapped at 1-km resolution using data from two nearly identical MODIS instruments on the *Terra* and *Aqua* satellites. This study uses only the *Terra* satellite's Collection-5 "MOD29" IST data. The MOD29 algorithm was developed to measure IST of snow and ice on the basis of the AVHRR heritage algorithm of Key and Haefliger (1992). MOD29 had been used successfully to map IST of sea ice but all land had been masked out. As a special product (Hall et al. 2012, 2013), the land/water mask was adjusted and now provides IST data using the MOD29 algorithm over Greenland as well as over sea ice. Improved geolocation data for the IST pixels were obtained using the "MOD03" product. The Greenland data are available online (http://modis-snow-ice.gsfc.nasa.gov/). For further information, see Hall et al. (2004) or Riggs et al. (2006), as well as additional documentation available online (https://nsidc.org/data/docs/daac/modis_v5/mod29_modis_terra_seaice_5min_swath_1km.gd.html).

The Greenland IST data use the standard MODIS 1-km-resolution cloud mask ("MOD35") that uses up to

14 spectral bands and multiple spectral and thermal tests to identify clouds (Ackerman et al. 1998, 2008; Liu et al. 2004). This product uses several cloud-detection tests to indicate a level of confidence that a pixel is clear or cloudy. For the MODIS data used in this study, changes were implemented that resulted in improvement in cloud masking during the polar night over snow and ice targets (Frey et al. 2008). These changes reduced the misidentification of cloud as clear but did not change the misidentification of clear pixels as cloud covered (Liu et al. 2004; Frey et al. 2008; Westermann et al. 2012; Østby et al. 2014). For the Greenland IST data near Summit that were used here, the conservative cloud tests in MOD35, called "confident clear," are used but have been considered to be overly conservative over snow and ice targets (Stroeve et al. 2006). Hall et al. (2013) document the need for additional editing of "clear" pixels that are too cold because of the presence of undetected clouds in the MOD35 product. Note that, of the 1883 days in our study period, ~29% of the days had no IST values for the Summit area, ~19% of the days had one IST value, ~35% of the days had two IST values, and ~17% of the days had three IST values (2536 IST values in total).

3. Method and results

The *Terra* MODIS-derived IST dataset (Riggs et al. 2006) and associated swath geolocation data were used to identify values that passed the confident-clear test and were within 3 km from the TAWO location. If multiple IST values were within this distance, only the closest observation was included in our analysis. These data were extracted for the period from July of 2008 through August of 2013. Using the 1-min-average data from TAWO, ±3-min-average T_A measurements were derived to bracket the times of the MODIS ISTs. This averaging period was chosen to provide a close correspondence to the well-defined data-acquisition times from MODIS. All data are recorded in UTC. Following some quality-control tests to identify possibly inaccurate T_A values that are typically associated with equipment issues at TAWO (only one 1-min data value was removed by looking for unusual excursions in the 1-min averages within the NOAA time series, but a small number of other days were reprocessed), the combined dataset was temporally aligned and then analyzed. In addition, the IST data were first analyzed without a filter and then with one, as discussed further below, that was designed to minimize the impact of expected cloud-affected values. In the following material, all data from 2008 to 2013 are plotted collectively, but individual years are summarized in Table 1.

a. T_A and IST data for 2008–13

The relationship between the ±3-min-average T_A and the contemporaneous IST data is shown in Fig. 1 for more than 2500 temperature comparisons. The red plus signs represent the full dataset in the scatterplot and show a fairly strong linear relationship across the temperature range from approximately 0° to less than −60°C. Note that this upper limit would obscure the positive temperatures associated with the rare melt event(s) in 2012 at Summit during 11–12 July. The trend of the regression line through all of the matched temperature values indicates that the expected slightly colder IST values range from just colder than the T_A observations at the upper part of the temperature range to ~5°C colder at the lower part of Summit's temperature range. As shown in Fig. 1, a number of outliers scatter significantly (>10°C) from the overall trend of the full dataset.

Because of this degree of scatter, it appears that some of the IST data are still cloud-affected or are otherwise anomalous despite the confident-clear cloud-masking procedure. Examination of Fig. 1 suggests that these outliers can be present throughout the annual temperature range. In general, IR-derived values affected by clouds will be substantially colder than the underlying ice-sheet surface, especially in the summer months (Hall et al. 2013), although there are some instances in which the IST is slightly warmer than the corresponding T_A value, possibly as a result of mixing of warmer air from aloft during storms (Miller 1956). While it is possible that some of the scatter is due to the in situ data, the NOAA Logan T_A sensor has been calibrated to ITS-90 standards using NOAA's protocols with reported temperatures at ±0.1°C accuracy. In addition, the standard deviations of all of the 1-min data used in the ±3-min averages in this study are typically (~98% of the time) less than 0.5°C (Fig. 2). The scatter shown in Fig. 2 indicates that temperature variability is more common at lower temperatures. The standard deviations were not plotted as error bars in Fig. 1 because most would not be visible. Table 1 provides an overall assessment of the uncertainty of the IST data relative to the T_A data.

To better resolve the expected cold bias in the IST values, a filter was applied to reduce the overall variability in the dataset. To dramatically reduce cloud-affected and other anomalous IST values, an IST–T_A ±5° filter that is based on the full dataset's linear regression was applied to the full dataset. This range was selected to leave the majority of the data available for the additional steps in the analysis but without unevenly influencing any part of the overall data range. The points that were within this filter range are indicated with blue

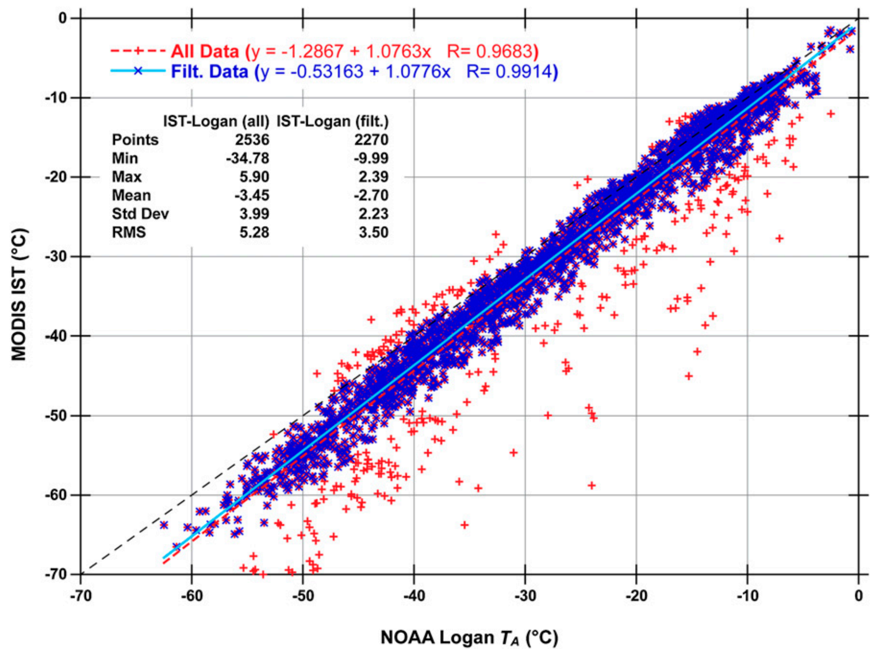

FIG. 1. Scatterplots of the temporally coincident 2008–13 IST and T_A data (±3-min averages). Linear regression lines are shown for all data (red symbols) and a subset of the data (blue symbols) after a ±5°C regression filter was applied. The dashed black line indicates where the two datasets would be equivalent. The rationale for the filter is discussed in the text, and the red-only points show the data that were excluded from further study. The blue regression line suggests that the IST–T_A difference is close to −0.5°C at freezing and is approximately −5°C at −60°C. Statistics for overall differences for the plotted data are shown. Generally similar results were obtained for each year of the study (see Table 1).

times signs in Fig. 1 and are represented by the blue regression line. Both datasets, denoted ''all'' and ''filt.,'' are summarized in Fig. 1 with IST–T_A difference statistics. Inspection of Fig. 1 indicates that this filter eliminates a number of outliers, most that are too cold but also some that are apparently too warm, from the remainder of the analysis (i.e., points with red plus signs only). The resulting blue linear regression line does not differ markedly from the initial regression through the raw data, but the filtering does reduce the mean difference by 0.75°C, and the variability is also reduced (see Fig. 1 and also the year-by-year data in Table 1). The filtered dataset is smaller by ~10% and is used for the rest of the study.

During our quality-control assessment of the NOAA T_A data, we observed that strong (>4°C) temperature changes can occur within some of the study's ±3-min averaging periods (see Fig. 2). These brief temperature swings can cause the standard deviation of the values to approach 2°C in some cases. Close examination of the minute-by-minute temperature data for the study period only identified one clearly anomalous 1-min observation that was edited from the NOAA time series. As a result of this analysis, however, 20 days of T_A data were identified of a total of 1883 days in the study period and were reprocessed to account for minor data issues. In any case, it is important to document that T_A can fluctuate relative to the essentially instantaneous IST data and that this may account for a minor amount of the scatter observed in Fig. 1.

b. MODIS IST variables

We used a number of ancillary parameters that are part of the MOD29 IST product in this study. First, we assessed the variability in IST–T_A differences due to the distance between the image pixel and the in situ values. As noted previously, offsets up to 3 km from the in situ data were accepted, as in some cases, the IST value over TAWO was not available typically due to the cloud mask. Figure 3 shows the IST–T_A differences for 2008–13 as a function of the offset distance. A weak relationship is indicated by the regression line, with the plot suggesting that most of the variability in the temperature differences is not a function of distance given the substantial variability within the 1-km distance from TAWO alone, indicated in Fig. 3. It is important to note that elevation variation is very small in the region as shown by unpublished ground-based GPS surveys

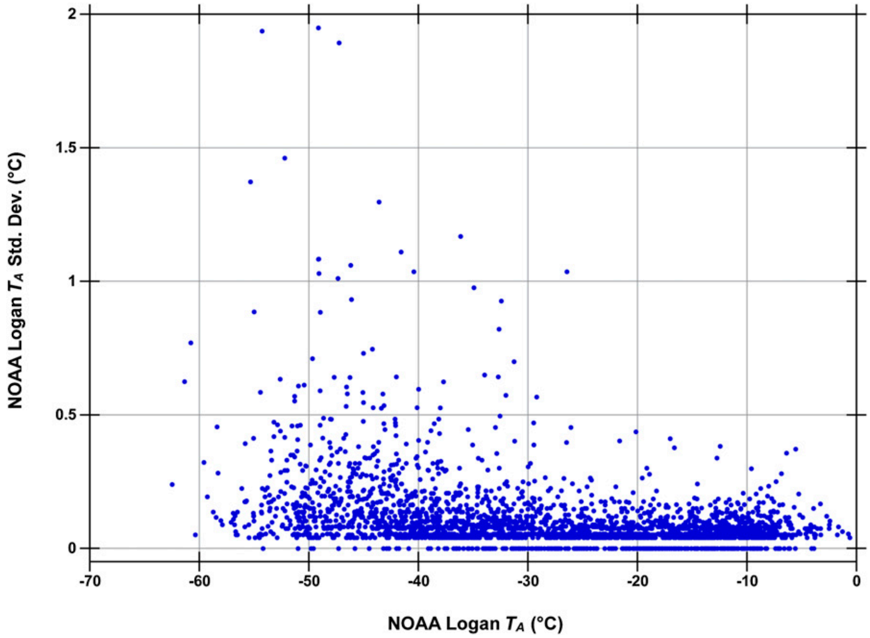

FIG. 2. Scatterplot showing the 2008–13 T_A variability (the standard deviation of all of the values in the ±3-min average) as a function of the mean temperature. In a few cases, temperature changes exceeding 5°C were documented within these short periods, leading to the larger standard deviation values. The "step" observed in the scatterplot is due to the 0.1°C reported resolution of the NOAA data.

conducted by Summit Station staff. The ice-sheet area around Summit has a homogeneous surface, as noted by Koenig and Hall (2010).

The sensor's-view zenith angle (SeZA) was also investigated because it can influence the IST–T_A difference. MODIS has a swath width of 2330 km; therefore, IST values for a specific location can be derived over a range of viewing geometries as the sensor orbits Earth. The sensor's SeZA is always recorded as a positive number, as shown in Fig. 4. The 2008–13 data suggest that slightly colder IST values are derived at larger angles from zenith. Results from previous research using AVHRR data (Dozier and Warren 1982) that show a temperature variation with SeZA are compatible with the results here. Because SeZA relative to a site like Summit is a function of satellite orbit and does not vary as a function of temperature through the year, this factor may contribute scatter but does not cause the overall cold bias that is apparent in Fig. 1.

The influence of the solar zenith angle (SoZA) on MODIS surface temperature retrievals was also investigated. A progressively greater offset between the IST and air temperatures toward the lower end of the temperature range (Fig. 1) suggests that the IST calibration at the low temperatures may be suspect. This is also illustrated in Fig. 5 with the 2008–13 IST–T_A differences plotted as a function of SoZA. Given Summit's northern latitude (72.58°N), this parameter varies considerably through the year with values that are greater than 90° indicating that the sun is below the horizon as is expected during the polar night. The trend of all of these data is also fairly consistent in each year of the study and shows colder IST values relative to T_A (more negative differences) as a function of higher SoZAs. A crucial result is that the magnitude of this regression (i.e., the offset of the temperature difference across the range of SoZA, ~4°C) is very close to the magnitude of the progressive IST cold bias observed in Fig. 1, with the offset increasing as temperatures fall over the temperature range expected during an annual cycle.

In addition, as shown by the data plotted in Fig. 5 and similarly for each year in the study, there appears to be more variability in IST–T_A differences about the trend at larger SoZAs. In fact, the linear regression mostly serves to illustrate the variation in the relationship of SoZA and temperature difference relative to the change from "day" to "night" cloud-filtering algorithms in the MODIS processing stream. Ackerman et al. (1998) document that the cloud-masking algorithm changes from day mode to night mode when SoZA exceeds 85°. This is close to where the data points in Fig. 5 change from having a fairly distinct linear trend despite some scattered values (<80°). although it is steeper than the overall regression, and begins to show increased variability (>80°).

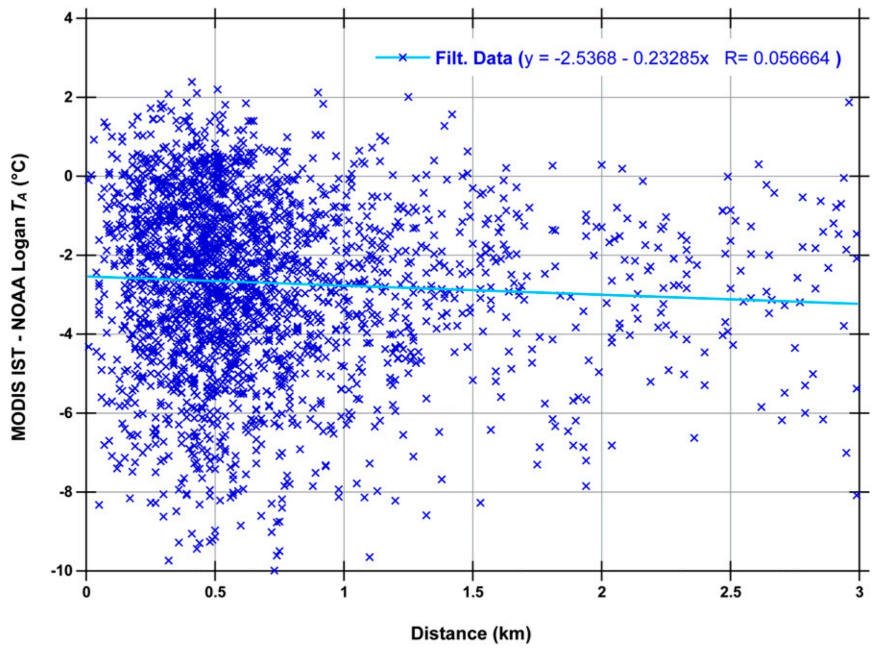

FIG. 3. Scatterplot of the 2008–13 IST–T_A differences as a function of the net distance between the MODIS pixel and the NOAA sensor location. A linear regression line shows little variation for data within 3 km. These data had the ±5° regression filter applied. The closest IST value was selected if more than one was available from the MODIS swath.

Even though the difference values continue to be generally to strongly negative at SoZAs that are greater than ~80°, the overall increase in scatter in Fig. 5 corroborates the known issue that the cloud-clearing algorithm is less reliable in near- to total darkness. This relationship within the filtered dataset likely contributes to the cold bias observed in Fig. 1, because SoZA does vary across the annual temperature cycle. This becomes especially problematic when monthly average ISTs are investigated because higher surface temperatures (which can occur under cloud cover) will not consistently be retrieved by MODIS because of cloud-cover obscuration of the ice-sheet surface (Hall et al. 2012).

4. Discussion

The multiyear comparisons presented here document that the observed cold bias (e.g., Figs. 1 and 5; Hall et al. 2008a) is not a static offset between T_A and IST over the full annual temperature range observed at Summit Station. The offset between contemporaneous air and ice-surface values is progressive across the full annual temperature range. It ranges from approximately −0.5°C at the upper end of the temperature range to as much as −5°C at −60°C after applying a modest additional test to reduce cloud-affected IST values. Further, this analysis reproduces a reported ~3°C cold bias between MODIS-derived skin and NOAA air temperatures (Koenig and Hall 2010) that was observed with data acquired from mid-November of 2008 to mid-February of 2009. Last, our analysis of ancillary IST parameters indicates a reason for the observed increasing cold bias as a function of decreasing temperatures at the Summit site. The combined impact of SoZA and reduced accuracy of cloud masking during the polar night appears to explain the overall observed cold bias (Fig. 5).

Work by Hudson and Brandt (2005) suggests that inversions can produce significant temperature gradients between the T_A sensor (nominal height of 2 m) and the ice surface, but it is not clear that these results are applicable to central Greenland. Work by Miller et al. (2013) at Summit indicates that there are variations in the frequency and intensity of inversions at Summit but does not detail their impact very close to the surface or other factors that can influence near-surface inversions. Our results (Fig. 1) suggest that while a seasonally varying "inversion effect" may be a factor it seems unlikely to lead to the smooth progression of the offset between IST and T_A values over the annual temperature range. Therefore, the progressive cold bias detailed in this analysis appears primarily to be a function of the SoZA when the MODIS data are acquired. A secondary factor appears to be the reduced ability to mask out

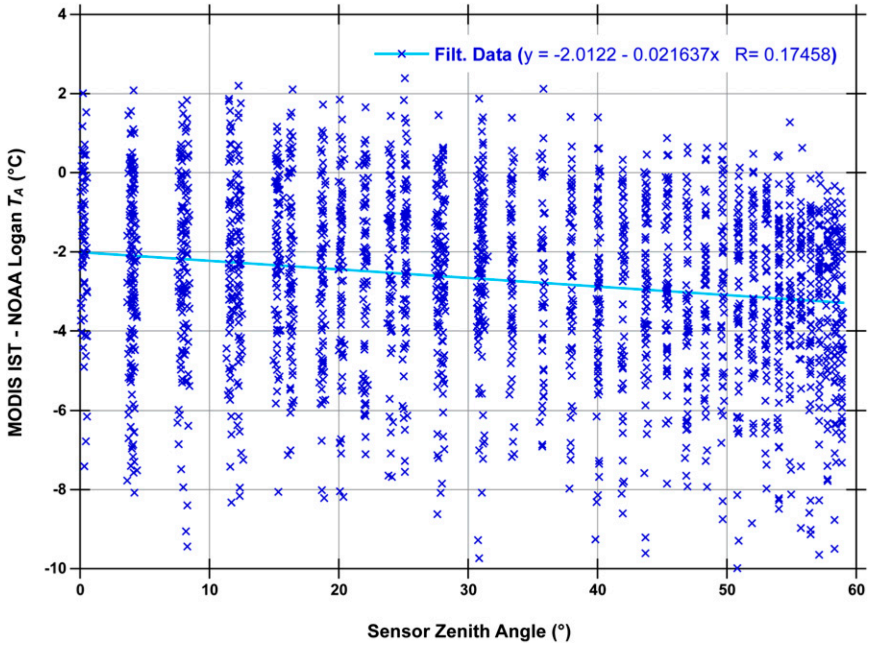

FIG. 4. Scatterplot of the 2008–13 IST–T_A differences as a function of angle between the MODIS sensor and the in situ data. The regression line suggests that there is a small decrease in IST as the angle increases. These data had the ±5° regression filter applied.

cloudy, and generally colder, MODIS pixels by the cloud-masking portion of the MOD29 algorithm; this becomes more common when the sun is close to or below the horizon. The effectiveness of the cloud-masking algorithm is reduced when it changes from day to night mode when SoZAs exceed 85° (Ackerman et al. 1998), and this is apparent in both the unfiltered and filtered temperature-difference data. This result suggests that improved cloud masking, although challenging during the polar night, would substantially improve the derived IST values for most users. Lesser factors such as the distance between the IST value and the in situ temperature site or the sensor's SeZA relative to the in situ data contribute some scatter to the IST–T_A relationship but do not control the progressive cold bias.

5. Conclusions

Analysis of the relationship between the TAWO 2-m T_A data and MODIS-derived IST values confirms that there is a progressive "cold bias" between the temporally coincident air and ice-surface observations near the GrIS's Summit Station. In addition, for temperatures that are closer to 0°C, IST values are closely compatible with contemporaneous (±3 min) T_A data. These datasets, compared during the period from 2008 to 2013, show that there is a difference of approximately −0.5°C at the upper end of the temperature range that increases to as much as −5° at −60°C. The offset is within the IST uncertainty at the upper end of the temperature range, with a larger offset and colder IST values relative to T_A averages increasing progressively over the annual temperature range. This offset appears to be largely a function of the MODIS data's SoZA and perhaps, to a lesser degree, the ability to reliably identify cloud-affected pixels by the cloud-masking algorithms. The impact of temperature inversions that can cause near-surface temperature gradients remains uncertain (e.g., Miller et al. 2013) and assessing their impact would require additional high-resolution observations at TAWO. The analysis results are consistent in each year of the study and are consistent with previous results obtained at Summit by Koenig and Hall (2010). The consistency of the relationship between T_A and IST suggests that an empirical correction may be used to refine the overall IST values to make them more compatible with T_A observations. Other sensors with IR bands, such as VIIRS and TIRS, would benefit from similar comparisons with NOAA's climate-quality temperature observations at Summit. Last, although we have identified some issues that IST users should consider, the bottom line is that the satellite IST observations have the consistency to provide knowledge of surface temperature of the GrIS that are useful for climate-modeling and climate-change studies.

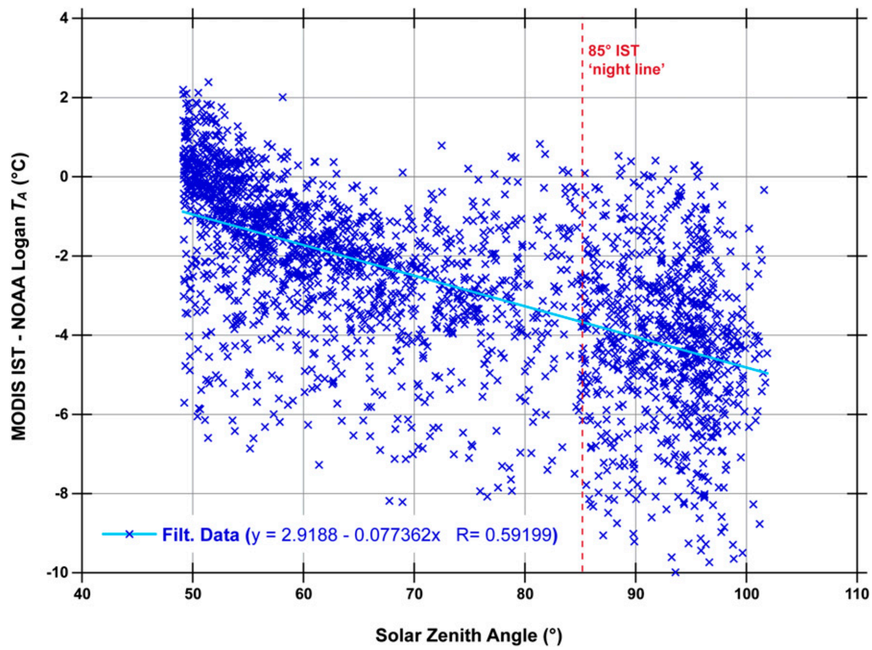

FIG. 5. Scatterplot of the 2008–13 IST–T_A differences as a function of the solar zenith angle relative to the IST location. The regression line is not an ideal model for these data but suggests that there is a distinct decrease in IST relative to T_A as the angle increases. These data had the $\pm5°$ regression filter applied. Additional structure in the plotted data is discussed in the text.

Acknowledgments. The authors thank the support staff at the Greenland Summit Station for helping to provide the in situ data necessary for this study. The T_A data were derived from NOAA's Earth System Research Laboratory Global Monitoring Division datasets. NASA's Cryospheric Sciences Program provided funding for the MODIS IST dataset as well as the work performed at NASA Goddard Space Flight Center (GSFC) and at University of Maryland, Baltimore County. Jack Xiong and Brian Wenny of the MODIS Characterization and Support Team at GSFC and George Riggs (Science Systems and Applications, Inc., at GSFC), provided additional insights on the IST data and MODIS products. We thank the editor and three anonymous reviewers for their comments and guidance that improved the final paper.

REFERENCES

Ackerman, S. A., K. I. Strabala, P. W. P. Menzel, R. A. Frey, C. C. Moeller, and L. E. Gumley, 1998: Discriminating clear sky from clouds with MODIS. *J. Geophys. Res.,* **103,** 32 141–32 157, doi:10.1029/1998JD200032.

——, R. E. Holz, R. Frey, E. W. Eloranta, B. Maddux, and M. McGill, 2008: Cloud detection with MODIS. Part II: Validation. *J. Atmos. Oceanic Technol.,* **25,** 1073–1086, doi:10.1175/2007JTECHA1053.1.

Box, J. E., 2002: Survey of Greenland instrumental temperature records: 1873–2001. *Int. J. Climatol.,* **22,** 1829–1847, doi:10.1002/joc.852.

——, X. Fettweis, J. C. Stroeve, M. Tedesco, D. K. Hall, and K. Steffen, 2012: Greenland Ice Sheet albedo feedback: Thermodynamics and atmospheric drivers. *Cryosphere,* **6,** 821–839, doi:10.5194/tc-6-821-2012.

Comiso, J. C., 2006: Arctic warming signals from satellite observations. *Weather,* **61** (3), 70–76, doi:10.1256/wea.222.05.

——, J. Yang, S. Honjo, and R. A. Krishfield, 2003: Detection of change in the Arctic using satellite and in situ data. *J. Geophys. Res.,* **108,** 3384, doi:10.1029/2002JC001347.

Cullather, R. I., S. M. J. Nowicki, B. Zhao, and M. J. Suarez, 2014: Evaluation of the surface representation of the Greenland Ice Sheet in a general circulation model. *J. Climate,* **27,** 4835–4856, doi:10.1175/JCLI-D-13-00635.1.

Dozier, J., and S. Warren, 1982: Effect of viewing angle on the infrared brightness temperature of snow. *Water Resour. Res.,* **18,** 1424–1434, doi:10.1029/WR018i005p01424.

Frey, R., S. Ackerman, Y. Liu, K. Strabala, H. Zhang, J. Key, and X. Wang, 2008: Cloud detection with MODIS. Part I: Improvements in the MODIS cloud mask for Collection 5. *J. Atmos. Oceanic Technol.,* **25,** 1057–1072, doi:10.1175/2008JTECHA1052.1.

Genthon, C., D. Six, V. Favier, M. Lazzara, and L. Keller, 2011: Atmospheric temperature measurement biases on the Antarctic Plateau. *J. Atmos. Oceanic Technol.,* **28,** 1598–1605, doi:10.1175/JTECH-D-11-00095.1.

Hall, D. K., J. Key, K. A. Casey, G. A. Riggs, and D. J. Cavalieri, 2004: Sea ice surface temperature product from MODIS. *IEEE Trans. Geosci. Remote Sens.,* **42,** 1076–1087, doi:10.1109/TGRS.2004.825587.

——, J. E. Box, K. A. Casey, S. J. Hook, C. A. Shuman, and K. Steffen, 2008a: Comparison of satellite-derived and in-situ observations of ice and snow surface temperatures over

Greenland. *Remote Sens. Environ.,* **112,** 3739–3749, doi:10.1016/j.rse.2008.05.007.

——, R. S. Williams Jr., S. B. Luthcke, and N. E. DiGirolamo, 2008b: Greenland Ice Sheet surface temperature, melt and mass loss: 2000–2006. *J. Glaciol.,* **54,** 81–93, doi:10.3189/002214308784409170.

——, S. V. Nghiem, C. B. Schaaf, N. E. DiGirolamo, and G. Neumann, 2009: Evaluation of surface and near-surface melt characteristics on the Greenland Ice Sheet using MODIS and QuikSCAT data. *J. Geophys. Res.,* **114,** F04006, doi:10.1029/2009JF001287.

——, J. C. Comiso, N. E. DiGirolamo, C. A. Shuman, J. R. Key, and L. S. Koenig, 2012: A satellite-derived climate-quality data record of the clear-sky surface temperature of the Greenland Ice Sheet. *J. Climate,* **25,** 4785–4798, doi:10.1175/JCLI-D-11-00365.1.

——, ——, ——, ——, J. E. Box, and L. S. Koenig, 2013: Variability in the surface temperature and melt extent of the Greenland Ice Sheet from MODIS. *Geophys. Res. Lett.,* **40,** 2114–2120, doi:10.1002/grl.50240.

Hanna, E., and Coauthors, 2014: Atmospheric and oceanic climate forcing of the exceptional Greenland Ice Sheet surface melt in summer 2012. *Int. J. Climatol.,* **34,** 1022–1037, doi:10.1002/joc.3743.

Hudson, S. R., and R. E. Brandt, 2005: A look at the surface-based temperature inversion on the Antarctic Plateau. *J. Climate,* **18,** 1673–1696, doi:10.1175/JCLI3360.1.

Key, J., and M. Haefliger, 1992: Arctic ice surface temperature retrieval from AVHRR thermal channels. *J. Geophys. Res.,* **97,** 5885–5893, doi:10.1029/92JD00348.

Koenig, L. S., and D. K. Hall, 2010: Comparison of satellite, thermochron and station temperatures at Summit, Greenland, during the winter of 2008/09. *J. Glaciol.,* **56,** 735–741, doi:10.3189/002214310793146269.

Liu, Y., J. Key, R. Frey, S. Ackerman, and W. P. Menzel, 2004: Nighttime polar cloud detection with MODIS. *Remote Sens. Environ.,* **92,** 181–194, doi:10.1016/j.rse.2004.06.004.

——, ——, and X. Wang, 2009: Influence of changes in sea ice concentration and cloud cover on recent Arctic surface temperature trends. *Geophys. Res. Lett.,* **36,** L20710, doi:10.1029/2009GL040708.

Lucas-Picher, P., M. Wulff-Nielsen, J. H. Christensen, G. Aðalgeirsdoìttir, R. Mottram, and S. B. Simonsen, 2012: Very high resolution regional climate model simulations over Greenland: Identifying added value. *J. Geophys. Res.,* **117,** D02108, doi:10.1029/2011JD016267.

Miller, D. H., 1956: The influence of snow cover on local climate in Greenland. *J. Meteor.,* **13,** 112–120, doi:10.1175/1520-0469(1956)013<0112:TIOSCO>2.0.CO;2.

Miller, N. B., D. D. Turner, R. Bennartz, M. D. Shupe, M. S. Kulie, M. P. Cadeddu, and V. P. Walden, 2013: Surface-based inversions above central Greenland. *J. Geophys. Res.,* **118,** 495–506, doi:10.1029/2012JD018867.

Nghiem, S. V., and Coauthors, 2012: The extreme melt across the Greenland Ice Sheet in 2012. *Geophys. Res. Lett.,* **39,** L20502, doi:10.1029/2012GL053611.

Østby, T. I., T. V. Schuler, and S. Westermann, 2014: Severe cloud contamination of MODIS land surface temperatures over an Arctic ice cap, Svalbard. *Remote Sens. Environ.,* **142,** 95–102, doi:10.1016/j.rse.2013.11.005.

Rennermalm, Å., and Coauthors, 2013: Understanding Greenland Ice Sheet hydrology using an integrated multi-scale approach. *Environ. Res. Lett.,* **8,** 015017, doi:10.1088/1748-9326/8/1/015017.

Riggs, G. A., D. K. Hall, and V. V. Salomonson, 2006: MODIS snow products user guide to Collection 5. NASA Goddard Space Flight Center Tech. Doc., 80 pp. [Available online at http://modis-snow-ice.gsfc.nasa.gov/uploads/sug_c5.pdf.]

Shuman, C. A., K. Steffen, J. E. Box, and C. R. Stearns, 2001: A dozen years of temperature observations at the Summit: Central Greenland automatic weather stations 1987–99. *J. Appl. Meteor.,* **40,** 741–752, doi:10.1175/1520-0450(2001)040<0741:ADYOTO>2.0.CO;2.

Stearns, C. R., and G. A. Weidner, 1990: Snow temperature profiles and heat fluxes measured on the Greenland crest by automatic weather stations. *Proc. Int. Conf. on the Role of Polar Regions on Climate Change,* Vol. 1, Fairbanks, AK, Geophysical Institute and the Center for Global Change and Arctic System Research, University of Alaska, Fairbanks, 223–226.

Steffen, K., and J. Box, 2001: Surface climatology of the Greenland Ice Sheet: Greenland Climate Network 1995–1999. *J. Geophys. Res.,* **106,** 33 951–33 964, doi:10.1029/2001JD900161.

Stroeve, J., and K. Steffen, 1998: Variability of AVHRR-derived clear-sky surface temperature over the Greenland Ice Sheet. *J. Appl. Meteor.,* **37,** 23–31, doi:10.1175/1520-0450(1998)037<0023:VOADCS>2.0.CO;2.

——, J. Box, and T. Haran, 2006: Evaluation of the MODIS (MOD10A) daily snow albedo product over the Greenland Ice Sheet. *Remote Sens. Environ.,* **105,** 155–171, doi:10.1016/j.rse.2006.06.009.

van den Broeke, M. R., P. Smeets, J. Ettema, C. van der Veen, R. van de Wal, and J. Oerlemans, 2008: Partitioning of melt energy and meltwater fluxes in the ablation zone of the west Greenland Ice Sheet. *Cryosphere,* **2,** 179–189, doi:10.5194/tc-2-179-2008.

——, C. J. P. P. Smeets, and R. S. W. van de Wal, 2011: The seasonal cycle and interannual variability of surface energy balance and melt in the ablation zone of the west Greenland Ice Sheet. *Cryosphere,* **5,** 377–390, doi:10.5194/tc-5-377-2011.

Wang, X., and J. Key, 2005a: Arctic surface, cloud, and radiation properties based on the AVHRR Polar Pathfinder dataset. Part I: Spatial and temporal characteristics. *J. Climate,* **18,** 2558–2574, doi:10.1175/JCLI3438.1.

——, and ——, 2005b: Arctic surface, cloud, and radiation properties based on the AVHRR Polar Pathfinder data set. Part II: Recent trends. *J. Climate,* **18,** 2575–2593, doi:10.1175/JCLI3439.1.

Warren, S. G., and R. E. Brandt, 2008: Optical constants of ice from the ultraviolet to the microwave: A revised compilation. *J. Geophys. Res.,* **113,** D14220, doi:10.1029/2007JD009744.

Westermann, S., M. Langer, and J. Boike, 2012: Systematic bias of average winter-time land surface temperatures inferred from MODIS at a site on Svalbard, Norway. *Remote Sens. Environ.,* **118,** 162–167, doi:10.1016/j.rse.2011.10.025.